ELSEVIER

Measurement 27 (2000) 231–239

Measurement

www.elsevier.com/locate/measurement

Propagation of uncertainty in a discrete Fourier transform algorithm

Giovanni Betta[a,*], Consolatina Liguori[a], Antonio Pietrosanto[b]

[a]*Department of Automation, Electromagnetism, Information Engineering and Industrial Mathematics, University of Cassino, Cassino (FR), Italy*

[b]*Department of Information Engineering and Electrical Engineering, University of Salerno, Fisciano (SA), Italy*

Received 15 July 1999; accepted 14 October 1999

Abstract

The problem of evaluating the uncertainty that characterises discrete Fourier transform output data is dealt with, using a method based on a 'white box' theoretical approach. The main sources of uncertainty (quantization, time jitter, microprocessor finite wordlength) are analysed obtaining equations useful to evaluate the uncertainty in both module and phase output values, for any hardware configuration and for any algorithm operating condition. The theoretical results, verified by both simulation and experimental tests, can be particularly useful for any designer and user of DFT-based instruments, since they allow the measurement configuration to be optimised with respect to the final uncertainty.

Keywords: Uncertainty analysis; DFT; FFT; Algorithm uncertainty

1. Introduction

More and more both commercial and custom measurement instruments are today based on the digital elaboration of measured data, with a consequent growing need for digital signal elaboration (DSE) algorithms in any application field. Besides the hardware configuration, the performance of these instruments strongly depends on the specific DSE algorithm, which may have influence on both bias and uncertainty of the output data [1]. Consequently, there is a great interest in setting up methods for DSE output bias and uncertainty evaluation, which allow both instrument designers and users to take into account also the software contribution to the metrological characteristics of the whole instrument [2–10].

In this framework, as far as frequency domain DSE algorithms (discrete and fast Fourier transform, DFT and FFT, algorithms) are concerned, numerous and valuable suggestions can be found in the literature. A world-wide discussion is open about deterministic errors that mainly cause bias in the results [11]. Other fundamental studies concern the bias effects of the chosen window [12], of asynchronous sampling, of the finite duration of the sampling impulses on frequency, amplitude, and phase estimations [13]. Together with these error analyses, tech-

*Corresponding author. Tel.: +39-776-299-673; fax +39-776-310-812.

E-mail addresses: betta@ing.unicas.it (G. Betta), liguori@ing.unicas.it (C. Liguori), pietrosa@diiie.unisa.it (A. Pietrosanto)

0263-2241/00/$ – see front matter
PII: S0263-2241(99)00068-8

niques or suitable elaboration are often suggested in order to reduce the final bias of the results (e.g. interpolation techniques, advanced windows [14–17]).

As to the uncertainty on DFT output data, no information is given on how input data uncertainty (e.g. arising from A/D converter quantization noise and sampling frequency jitter) propagates through the algorithm. Consequently, nothing is said either about spectrum amplitude and phase uncertainty or about its analytical relationship with measurement parameters such as number of samples, sampling frequency or A/D converter (ADC) number of bits.

In this paper, the authors, on the basis of their previous experiences in this field [18–22], tackle the problem of analytical evaluation of DFT and FFT output data uncertainty, according to the *Guide to the Expression of Uncertainty in Measurement* (GUM) [23]. They adopt a white box approach already proposed and applied on some time domain DSE algorithms [21,22]. This approach allows a preventive evaluation of DSE algorithm output data uncertainty to be carried out once the algorithm and the input data uncertainty analytical models are known. In particular, ADC quantization noise, sampling frequency jitter, and microprocessor finite wordlength will be considered. The obtained analytical formulae are then numerically verified by simulation tests and experimentally validated on real hardware configurations.

2. Measurement algorithm and sources of uncertainty

2.1. The measurement algorithm

The DFT of an N-point sequence $\{x(n)\}$ is defined as:

$$X(k) = \frac{1}{N}\sum_{n=0}^{N-1} x(n)\, e^{-jk\beta_n} \quad k = 0 \ldots N-1 \tag{1}$$

where $\beta_n = 2\pi n/N$ and a synchronous sampling is assumed. Having posed:

$$\begin{cases} R(k) &= \displaystyle\sum_{n=0}^{N-1} x(n)\cos(k\beta_n) \\ I(k) &= \displaystyle\sum_{n=0}^{N-1} x(n)\sin(k\beta_n) \end{cases} \tag{2}$$

the following states: $X(k) = (R(k) - jI(k))/N$ and, consequently, the module $M(k)$ and the phase $\varphi(k)$ of each frequency domain sample $X(k)$ are given, respectively, by:

$$M(k) = \frac{1}{N}\sqrt{R^2(k) + I^2(k)} \tag{3}$$

$$\varphi(k) = \operatorname{arctg}\left(-\frac{I(k)}{R(k)}\right). \tag{4}$$

2.2. Uncertainty due to quantization

Each sample $x(n)$ is affected by an uncertainty equal to U_q, due to the quantization process, performed by a real ADC with B effective bit number and range V_{Range}; this uncertainty can be modelled as a zero mean random variable with standard deviation [24]:

$$U_q = V_{\text{Range}} \cdot 2^{-B}/\sqrt{12}. \tag{5}$$

2.3. Uncertainty due to jitter

In an actual ADC, the sampling time τ is not constant for a number of reasons (e.g. noise on the sampling impulse, uncertainty on the Sample and Hold aperture time, clock instability). This phenomenon, known as time jitter, can be modelled by adding to each ideal sampling instant t_n a random variable δ_n uniformly distributed in the interval $[-J_\tau, +J_\tau]$, with zero mean and variance $E[\delta_n^2] = J_\tau^2/3$ [6]. As a consequence, the nth sampled value $x(n)$ has to be considered as a random variable. In particular it can be represented as the sum between the ideal value and a zero-mean uniformly distributed random variable α_n. Consequently each sampled value $x(n)$ is affected by an uncertainty equal to the standard deviation of the variable α_n. Approximating $x(t)$ in the interval $[n\tau - J_\tau, n\tau + J_\tau]$ with a linear function, the α_n range can be estimated equal to $[-a_n J_\tau, +a_n J_\tau]$ and its standard deviation is

$$U_{J_n} = \sqrt{E[\alpha_n^2]} = a_n \cdot J_\tau/\sqrt{3} \tag{6}$$

where a_n is the first derivative of $x(t)$ in the considered point.

2.4. Uncertainty due to the microprocessor finite wordlength

Uncertainty in binary arithmetic operations depends on whether the arithmetic is fixed or floating point. In fact, fixed-point addition does not increase the wordlength if the sum is guaranteed to be less than unity. On the other hand, in floating-point arithmetic both addition and multiplication involve rounding, hence giving rise to a quantization uncertainty.

2.4.1. Floating-point

The uncertainties introduced by floating-point operations are modelled as follows [25,26]:

$$fl(x \cdot y) = (x \cdot y) \cdot (1 + \gamma) \tag{7}$$

$$fl(x + y) = (x + y)(1 + \eta) \tag{8}$$

where γ and η are zero mean random variables, independent on x, y, and $(x + y)$ or $(x \cdot y)$, respectively, uniformly distributed in the range $[-2^{-B_M}, 2^{-B_M}]$ where B_M is the number of bits used to represent the mantissa and their standard deviations were found to be equal to:

$$U_{fl\_m} = \sqrt{E[\gamma^2]} \approx \sqrt{0.18 \cdot 2^{-2 \cdot B_M}} \tag{9}$$

$$U_{fl\_a} = \sqrt{E[\eta^2]} \approx \sqrt{p \cdot 0.18 \cdot 2^{-2 \cdot B_M}} \tag{10}$$

where p is a factor depending on the probability of there being a rounding in an addition ($p = 0.5$–0.6) [27].

2.4.2. Fixed-point

The multiplication is modelled as:

$$fx(x \cdot y) = x \cdot y + \varepsilon \tag{11}$$

where ε is zero mean random variables, independent on x, y, and $(x \cdot y)$, uniformly distributed in the range $[-2^{-B_x}, 2^{-B_x}]$, with B_x the fixed wordlength, and variance $E[\varepsilon^2] = 2^{-2 \cdot B_x}/12$ [28,29]. Consequently, each multiplication will add an uncertainty equal to:

$$U_{fx} = \sqrt{2^{-2 \cdot B_x}/12}. \tag{12}$$

Moreover, in order to assure the absence of overflows in additions, a preliminary division by the number of addendum must be carried out. This operation will cause both an additional division by N and a correspondent resolution reduction that must be taken into account in the algorithm uncertainty estimation.

3. Theoretical estimation of uncertainty

To show the effect of the different uncertainty sources on the final measurement results, the different sources were analysed separately and with reference to both real and imaginary components of DFT components. Finally the effect on module and phase of each DFT sample are evaluated.

3.1. Quantization

The absolute uncertainty on $R(k)$ and $I(k)$ can be estimated by applying the uncertainty propagation law to Eq. (2), obtaining:

$$\begin{cases} U^2_{R(k)}|_q = \sum_{m=0}^{N-1} \left(\frac{\partial R(k)}{\partial x(m)} \right)^2 U^2_{x(m)} = \sum_{m=0}^{N-1} \cos^2(k\beta_m) U^2_q \\ U^2_{I(k)}|_q = \sum_{m=0}^{N-1} \left(\frac{\partial I(k)}{\partial x(m)} \right)^2 U^2_{x(m)} = \sum_{m=0}^{N-1} \sin^2(k\beta_m) U^2_q \end{cases} \tag{13}$$

Being:

$$\begin{cases} \sum_{m=0}^{N-1} \cos^2(k\beta_m) = \begin{cases} N & \text{for } k = 0 \\ \frac{N}{2} & \text{for } k \neq 0 \end{cases} \\ \sum_{m=0}^{N-1} \sin^2(k\beta_m) = \begin{cases} 0 & \text{for } k = \text{'0} \\ \frac{N}{2} & \text{for } k \neq 0 \end{cases} \end{cases}$$

Eq. (13) becomes:

$$\begin{cases} U^2_{R(k)}|_q = \begin{cases} NU^2_q & \text{for } k = 0 \\ \frac{N}{2} U^2_q & \text{for } k \neq 0 \end{cases} \\ U^2_{I(k)}|_q = \begin{cases} 0 & \text{for } k = 0 \\ \frac{N}{2} U^2_q & \text{for } k \neq 0 \end{cases} \end{cases} \tag{14}$$

3.2. Time jitter

The uncertainty due to the time jitter is equal to:

$$\begin{cases} U^2_{R(k)}\big|_J &= \sum_{m=0}^{N-1}\left(\frac{\partial R(k)}{\partial x(m)}\right)^2 U^2_{J_m} = \sum_{m=0}^{N}\cos^2(k\beta_m)U^2_{J_m} \\ U^2_{I(k)}\big|_J &= \sum_{m=0}^{N-1}\left(\frac{\partial I(k)}{\partial x(m)}\right)^2 U^2_{J_m} = \sum_{m=0}^{N}\sin^2(k\beta_m)U^2_{J_m} \end{cases} \tag{15}$$

where the value of U_{J_m} depends on the signal slope in the sampling instant according to Eq. (6).

3.3. Microprocessor finite wordlength

3.3.1. Floating-point

On the basis of the introduced finite wordlength uncertainties, and considering the multiplication uncertainties only on $x(n)\cdot\cos(k\beta_n)$ and $x(n)\cdot\sin(k\beta_n)$, the following equations state:

$$\begin{cases} fl[R(k)]_m &= \sum_{n=0}^{N-1} x(n)\cdot\cos(k\beta_n)\cdot(1+\gamma_n) \\ fl[I(k)]_m &= \sum_{n=0}^{N-1} x(n)\cdot\sin(k\beta_n)\cdot(1+\gamma_n) \end{cases} \tag{16}$$

where γ_n is the uncertainty introduced by the nth multiplication.

As to additions, with easy mathematical passages and neglecting the second order terms, the following equations state:

$$\begin{cases} fl[R(k)]_a &= \sum_{n=0}^{N-1} x(n)\cdot\cos(k\beta_n) + \sum_{n=1}^{N-1}\eta_n\sum_{i=0}^{n} x(i)\cdot\cos(k\beta_i) \\ fl[I(k)]_a &= \sum_{n=0}^{N-1} x(n)\cdot\sin(k\beta_n) + \sum_{n=1}^{N-1}\eta_n\sum_{i=0}^{n} x(i)\cdot\sin(k\beta_i) \end{cases} \tag{17}$$

where η_n is the uncertainty introduced by the nth addition.

By applying the GUM procedure to the above equations, it is possible to obtain:

$$\begin{cases} U^2_{R(k)}\big|_{fl\_m} &= \sum_{m=0}^{N-1}\left(\frac{\partial R(k)}{\partial \gamma_m}\right)^2 U^2_{fl\_m} = \sum_{m=0}^{N-1}(x(m)\cos(k\beta_m))^2 U^2_{fl\_m} \\ U^2_{I(k)}\big|_{fl\_m} &= \sum_{m=0}^{N-1}\left(\frac{\partial I(k)}{\partial \gamma_m}\right)^2 U^2_{fl\_m} = \sum_{m=0}^{N-1}(x(m)\sin(k\beta_m))^2 U^2_{fl\_m} \end{cases} \tag{18}$$

$$\begin{cases} U^2_{R(k)}\big|_{fl\_a} &= \sum_{m=1}^{N-1}\left(\frac{\partial R(k)}{\partial \eta_m}\right)^2 U^2_{fl\_a} = \sum_{m=1}^{N-1}\left(\sum_{i=1}^{m} x(i)\cos(k\beta_i)\right)^2 U^2_{fl\_a} \\ U^2_{I(k)}\big|_{fl\_a} &= \sum_{m=1}^{N-1}\left(\frac{\partial I(k)}{\partial \eta_m}\right)^2 U^2_{fl\_a} = \sum_{m=1}^{N-1}\left(\sum_{i=1}^{m} x(i)\sin(k\beta_i)\right)^2 U^2_{fl\_a} \end{cases} \tag{19}$$

3.3.2. Fixed-point

By considering the uncertainties introduced by fixed point multiplications, it is possible to write:

$$\begin{cases} fx[R(k)]_m &= \sum_{n=0}^{N-1}[x(n)\cdot\cos(k\beta_n)+\varepsilon_n] \\ fx[I(k)]_m &= \sum_{n=0}^{N-1}[x(n)\cdot\sin(k\beta_n)+\varepsilon_n] \end{cases} \tag{20}$$

Starting from this equation, the following is obtained:

$$\begin{cases} U^2_{R(k)}\big|_{fx} &= \sum_{m=0}^{N-1}\left(\frac{\partial R(k)}{\partial \sigma_m}\right)^2 U^2_{fx} = NU^2_{fx} \\ U^2_{I(k)}\big|_{fx} &= \sum_{m=0}^{N-1}\left(\frac{\partial I(k)}{\partial \sigma_m}\right)^2 U^2_{fx} = NU^2_{fx} \end{cases}. \tag{21}$$

The above equations highlight that the absolute uncertainty is independent on k (e.g. on the tone frequency) and on the amplitude of the tone.

3.4. Uncertainty on module and phase

By applying the GUM procedure to Eqs. (3) and (4), general expressions for uncertainty on module and phase can be obtained:

$$U^2_{M(k)} = \frac{1}{N^4M^2(k)}[R^2(k)U^2_{R(k)} + I^2(k)U^2_{I(k)} + 2R(k)I(k)U(R(k),I(k))] \tag{22}$$

$$U^2_{\varphi(k)} = \frac{1}{N^4M^4(k)}[I^2(k)U^2_{R(k)} + R^2(k)U^2_{I(k)} - 2R(k)I(k)U(R(k),I(k))]. \tag{23}$$

These equations can then be specified by introducing the uncertainties due to the different sources previously evaluated obtaining the final equations useful for estimating the effect on module and phase of the different uncertainty sources.

3.4.1. Quantization

Being

$$U(R(k),I(k)) = \sum_{m=0}^{N-1} \frac{\partial R(k)}{\partial x_m} \cdot \frac{\partial I(k)}{\partial x_m} \cdot U^2_{x(m)} = \sum_{m=0}^{N-1} \cos(k\beta_m) \cdot \sin(k\beta_m) \cdot U^2_{x(m)} \quad (24)$$

and $\Sigma_{m=0}^{N-1} \cos(k\beta_m) \cdot \sin(k\beta_m) = 0$ for each k, the following equations can be derived:

$$U^2_{M(k)}|_q = \begin{cases} \frac{1}{N} U_q^2 & \text{for } k = 0 \\ \frac{1}{2N} U_q^2 & \text{for } k \neq 0 \end{cases} \quad (25)$$

$$U^2_{\varphi(k)}|_q = \begin{cases} \text{if } x \text{ real } \varphi(0) = 0 & \text{for } k = 0 \\ \frac{1}{2N \cdot M^2(k)} U_q^2 & \text{for } k \neq 0 \end{cases} \quad (26)$$

Eq. (25) clearly highlights that the absolute uncertainty on the module depends only on the uncertainty on each sample $x(n)$, which depend on the effective number of bits of the ADC, and on the number of points N used by the DFT algorithm. In particular, the uncertainty decreases with the increase of both N and ADC bit number.

Analogously for the phase, an inverse proportionality with N is evidenced. On the other hand, an inverse proportionality with $M(k)^2$ is evidenced. In other words, different tones with the same amplitude are affected by the same absolute uncertainty on the phase.

In any case the quantization effect does not depend on the signal dynamic, having assumed the effective number of bits of the ADC to be a constant in the operating frequency range.

3.4.2. Jitter

By introducing Eqs. (15) and (24), in Eqs. (22) and (23), the following equations can be derived:

$$U^2_{M(k)}|_J = \frac{1}{N^4 M^2(k)} \left[R^2(k) \sum_{m=0}^{N-1} \cos^2(k\beta_m) U^2_{J_m} + I^2(k) \sum_{m=0}^{N-1} \sin^2(k\beta_m) U^2_{J_m} + 2R(k)I(k) \sum_{m=0}^{N-1} \sin(k\beta_m) \cos(k\beta_m) U^2_{J_m} \right] \quad (27)$$

$$U^2_{\varphi(k)}|_J = \frac{1}{N^4 M^4(k)} \left[I^2(k) \sum_{m=0}^{N-1} \cos^2(k\beta_m) U^2_{J_m} + R^2(k) \sum_{m=0}^{N-1} \sin^2(k\beta_m) U^2_{J_m} + 2R(k)I(k) \sum_{m=0}^{N-1} \sin(k\beta_m) \cos(k\beta_m) U^2_{J_m} \right]. \quad (28)$$

These formulae clearly evidence an inverse proportionality with powers of both the number of points N and the sample module $M(k)$. The above formula can be simplified by considering $U^2_{J_m}$ constant and equal to its maximum value. In this case, Eqs. (27) and (28) become equal to Eqs. (25) and (26).

3.4.3. Microprocessor finite wordlength

By introducing in Eqs. (22) and (23) the results of Eqs. (18), (19) and (21) and taking into account that $R(k)$ and $I(k)$ are uncorrelated with respect to this kind of uncertainty source, the following equations can be easily derived:

$$U^2_{M(k)}|_{fl\_m} = \frac{1}{N^4 M^2(k)} \left(R^2(k) \sum_{m=0}^{N-1} (x(m)\cos(k\beta_m))^2 U^2_{fl\_m} + I^2(k) \sum_{m=0}^{N-1} (x(m)\sin(k\beta_m))^2 U^2_{fl\_m} \right) \quad (29)$$

$$U^2_{\varphi(k)}|_{fl\_m} = \frac{1}{N^4 M^4(k)} \left(I^2(k) \sum_{m=0}^{N-1} (x(m)\cos(k\beta_m))^2 U^2_{fl\_m} + R^2(k) \sum_{m=0}^{N-1} (x(m)\sin(k\beta_m))^2 U^2_{fl\_m} \right) \quad (30)$$

$$U^2_{M(k)}|_{fl\_a} = \frac{1}{N^4 M^2(k)} \left(R^2(k) \sum_{m=1}^{N-1} \left(\sum_{i=0}^{m} x(i)\cos(k\beta_i) \right)^2 U^2_{fl\_a} + I^2(k) \sum_{m=1}^{N-1} \left(\sum_{i=0}^{m} x(i)\sin(k\beta_i) \right)^2 U^2_{fl\_a} \right) \quad (31)$$

$$U^2_{\varphi(k)}\big|_{fl\_a} = \frac{1}{N^4 M^4(k)}\left(I^2(k)\sum_{m=1}^{N-1}\left(\sum_{i=0}^{m} x(i)\cos(k\beta_i)\right)^2 U^2_{fl\_a} + R^2(k)\sum_{m=1}^{N-1}\left(\sum_{i=0}^{m} x(i)\sin(k\beta_i)\right)^2 U^2_{fl\_a}\right) \quad (32)$$

$$U^2_{M(k)}\big|_{fx} = \frac{1}{N}\cdot U^2_{fx} \quad (33)$$

$$U^2_{\varphi(k)}\big|_{fx} = \frac{1}{NM^2(k)}\cdot U^2_{fx}. \quad (34)$$

3.5. Some considerations about the obtained theoretical results

A practical evaluation of the obtained theoretical results requires the definition of some parameters concerning the hardware configuration (number of effective bits, full scale and time jitter of the A/D converter, arithmetic and wordlength of the microprocessor), the operative condition (sampling frequency, number of elaborated points) as well as the characteristics of the input signal (spectral content). As an example, having fixed the characteristics of the input signal (50 Hz sinusoid with 0.7 V amplitude), the range of the A/D (± 1 V), and the frequency resolution of the DFT algorithm (6.25 Hz),

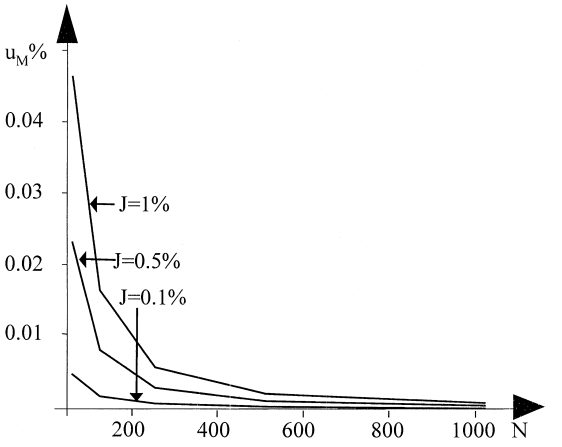

Fig. 2. Relative percentage uncertainty u_M% versus the elaboration point number (N), for different values of the time jitter J, expressed as a percentage of the sampling period.

Figs. 1–3 report the relative percentage uncertainty evolution for the module of the signal harmonic ($M(k)$ with $k = 8$) for different hardware configuration and operating conditions. In particular, Fig. 1 reports this uncertainty in function of the number of elaborated points (N) for different ADC number of bits, Fig. 2 reports the uncertainty evolution for different values of the time jitter, and Fig. 3 reports the relative percentage uncertainty in function of the number of elaborated points (N) for different micro-

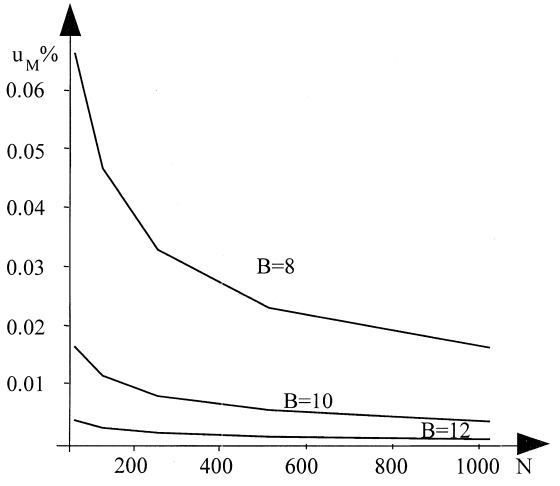

Fig. 1. Relative percentage uncertainty u_M% versus the elaboration point number (N), for different values of the A/D bit number (B).

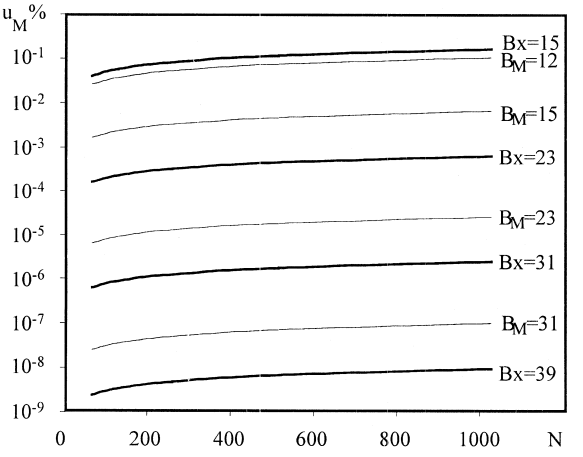

Fig. 3. Relative percentage uncertainty u_M% versus the elaboration point number (N), for fixed-point (bold lines) and floating-point (thin lines) arithmetic, and for different wordlength.

processors, adopting fixed- (bold line) or floating-point (thin line) arithmetic.

By comparing these figures, it is evident that the main source of uncertainty in the DFT algorithm is the quantization one, comparable only with fixed-point effects for lower number of bits of mantissa.

4. Numerical simulation and experimental validation

Numerical simulation was carried out with the aim of verifying the theoretical results in terms of correctness of the performed analytical analysis. In particular, the simulation, carried out in the Matlab environment, consists in introducing, on the input data and in the algorithm, the same uncertainties considered in the theoretical approach and in running the algorithm [30], for each chosen hardware and software configuration, a number of times suitable for a statistical uncertainty evaluation. The so obtained results are in very good agreement with the theoretical ones.

The experimental validation is focused in verifying the correctness of uncertainty models assumed in the previous analyses. The test signal (50 Hz sinusoid with amplitude equal to 70% of the ADC full-scale) were supplied by an arbitrary waveform generator AWG2020 by Tektronix, also used as a reference. Measurements were carried out by different measurement stations, whose main characteristics are summarised in the following

(a) ADC by Burr-Brown (16 nominal bit, 10.3 effective bit, 200 kHz maximum sampling frequency, 1.6 kHz sampling frequency used, ±3.1 V input range, clock stability <1 ppm)+ TMS320C40 DSP by Texas Instrument with 32 bit floating-point arithmetic ($B_M = 23$);
(b) digital oscilloscope TDS520 by Tektronix (8 nominal bit, 7.6 effective bit, 500 MHz maximum sampling frequency, 1 kHz sampling frequency used, ±2 V input range, clock stability <1 ppm)+TMS320C50 DSP by Texas Instrument with 16 bit fixed-point arithmetic ($B_x = 15$);
(c) ADC of the MCS-96 microcontroller by Intel (10 nominal bit, 7 effective bit, 8 kHz maximum sampling frequency, 800 Hz sampling frequency used, ±2.5 V input range, software clock with a programmable jitter 1/1000+MCS-96 CPU with 16 bit floating-point arithmetic ($B_M = 11$).

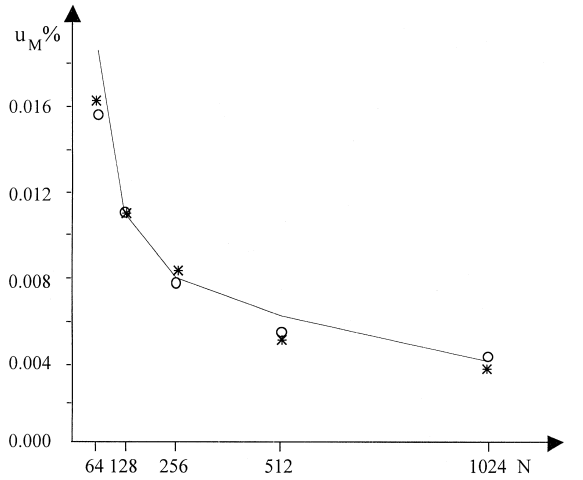

Fig. 4. Comparison between theoretical (line), simulation (*) and experimental (○) results with reference to the measurement station (a).

Figs. 4–6, corresponding to (a), (b), and (c) measurement stations, respectively, highlight a general good agreement among all the three phases of the proposed method. Only the experimental data of Fig. 6 result in an underestimation of the uncertainty;

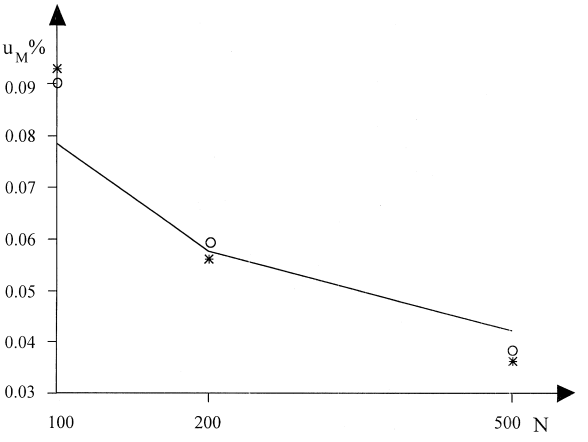

Fig. 5. Comparison between theoretical (line), simulation (*) and experimental (○) results with reference to the measurement station (b).

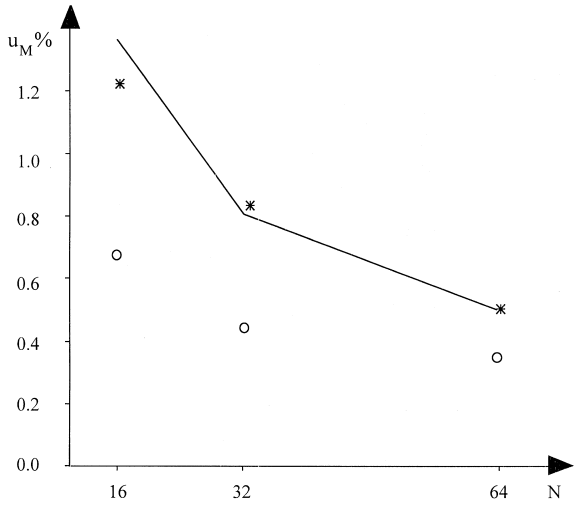

Fig. 6. Comparison between theoretical (line), simulation (*) and experimental (○) results with reference to the measurement station (c).

this is due to the time jitter model used that is based on a worst-case assumption.

5. Conclusions

The problem of output uncertainty estimation in DFT algorithms is tackled applying a 'white-box' approach based on a theoretical uncertainty evaluation, followed by both a numerical validation and an experimental verification.

The obtained analytical relationships between the algorithm output combined uncertainty and measurement parameters highlight as the most evident result that the main source of uncertainty in DFT algorithm is the quantization one, comparable only with fixed-point effects for lower number of bits of mantissa.

Experimental tests on a number of real DSP-based measurement stations confirm the possibility of a priori evaluating the uncertainty of digital elaboration algorithm, if all the sources of uncertainty are known and correctly modelled.

Acknowledgements

The authors wish to thank Ing. Roberto Petrillo for help given during this work.

References

[1] S. Sartori, A. Balsamo, Principles of calibration of intelligent instruments, in: Proceedings of XIII IMEKO World Congress, Torino, Italy, 1994, pp. 887–892.
[2] J. Kok, Validation of metrology software, in: Proceedings of I Workshop Advanced Mathematical Tools for Metrology, Torino, Italy, 1993, pp. 231–238.
[3] M.G. Cox, Graded reference data sets and performance profiles for testing software used in metrology, in: Proceedings of III Workshop Advanced Mathematical Tools for Metrology, Singapore, 1997, pp. 43–55.
[4] D. Richter, Software quality assurance in metrology, in: Proceedings of I Workshop Advanced Mathematical Tools for Metrology, Torino, Italy, 1993, pp. 255–262.
[5] V. Friedman, A zero crossing algorithm for the estimation of the frequency of a single sinusoid white noise, IEEE Trans. Signal Process. 42 (6) (1994) 1565–1569.
[6] S.S. Awad, The effects of accumulated timing jitter on some sine wave measurement, IEEE Trans. Instrum. Measur. 44 (5) (1995) 945–951.
[7] I. Kollar, Bias of mean value and mean square value measurements based on quantized data, IEEE Trans. Instrum. Measur. 43 (5) (1994) 733–739.
[8] J. Xi, J.F. Chicaro, A new algorithm for improving the accuracy of periodic signal analysis, IEEE Trans. Instrum. Measur. 45 (4) (1996) 827–831.
[9] N. Al-Dhahir, J.M. Cioffi, On the uniform ADC bit precision and clip level computation for gaussian signal, IEEE Trans. Signal Process. 44 (2) (1996) 434–438.
[10] L. Cristaldi, A. Ferrero, R. Ottoboni, Test and validation procedures for digital instruments for the measurement of electric power components, in: Proceedings of XIII IMEKO World Congress, Torino, Italy, 1994, pp. 673–678.
[11] R.I. Becker, N. Morrison, The errors in FFT estimation of the Fourier transform, IEEE Trans. Signal Process. 44 (8) (1996) 2073–2077.
[12] J. Harris, On the use of windows for harmonic analysis with the discrete Fourier transform, IEE Proc. 66 (1) (1978) 51–82.
[13] A.V. Oppenheim, R.W. Schafer, Discrete Time Signal Processing, Prentice-Hall, Englewood Cliffs, 1989.
[14] G. Andria, M. Savino, A. Trotta, Windows and interpolation algorithms to improve electrical measurement accuracy, IEEE Trans. Instrum. Measur. 88 (4) (1989) 856–863.
[15] C. Offelli, D. Petri, Interpolation techniques for real-time multifrequency waveform analysis, IEEE Trans. Instrum. Measur. 39 (1) (1990) 106–111.
[16] C. Offelli, D. Petri, The influence of windowing on the accuracy of multifrequency signal parameter estimation, IEEE Trans. Instrum. Measur 41 (2) (1992) 256–261.
[17] P. Daponte, C. Liguori, A. Pietrosanto, Real time harmonic analysis by multiple deep dip windows, in: Proceedings of IMEKO TC-4 International Symposium, Prague, Czech Republic, 1995, pp. 609–613.
[18] A. Bernieri, G. Betta, L. Sansone, Finite wordlength effect in a SISO identification algorithm, in: Proceedings of IMACS World Congress, Dublin, Ireland, 1991, pp. 1300–1303.

[19] G. Betta, L. Sansone, Analysis of error propagation in a recursive identification algorithm, in: Proceedings of XII IMEKO World Congress, Beijing, China, 1991, pp. 113–117.
[20] A. Bernieri, G. Betta, M. D'apuzzo, L. Sansone, Error analysis in a recursive identification algorithm, Measurement 13 (1994) 183–190.
[21] G. Betta, C. Liguori, A. Pietrosanto, Uncertainty analysis in digital signal processing algorithms, in: Proceedings of XIV IMEKO World Congress, Tampere, Finland, Vol. IVa, 1997, pp. 267–273.
[22] G. Betta, C. Liguori, A. Pietrosanto, A structured approach to estimate the measurement uncertainty in digital signal elaboration algorithms, IEE Proc. Part A Sci. Measur. Technol. 146 (1) (1999) 21–26.
[23] BIPM, IEC, IFCC, ISO, IUPAC, IUPAP, OIML, Guide to the Expression of Uncertainty in Measurement, 1993.
[24] B. Liu, Effect of finite wordlength on the accuracy of digital filters — a review, IEEE Trans. Circuit Theory 18 (6) (1971) 670–677.
[25] K. Kalliojarvi, J. Astola, Roundoff errors in block-floating-point system, IEEE Trans. Signal Process. 44 (4) (1996) 783–790.
[26] I. Pitas, M. Strintzis, Floating-point error analysis of two dimensional Fast Fourier Transform algorithms, IEEE Trans. Circuits Syst. 35 (1) (1988) 112–115.
[27] T. Kaneko, B. Liu, On local roundoff errors in floating-point arithmetic, J. Assoc. Comput. Machinery 20 (3) (1973) 391–398.
[28] C.G. Sampson, V.U. Reddy, Fixed point error analysis of the normalized ladder algorithm, IEEE Trans. Acoustic Speech Signal Process. 31 (5) (1983) 1177–1191.
[29] S.H. Ardalan, S.T. Alexander, Fixed-point roundoff error analysis of the exponentially windowed RLS algorithm for time varying systems, IEEE Trans. Acoustic Speech Signal Process. 35 (6) (1987) 770–783.
[30] V.V. Vujicic, Z.M. Ranic, A simulation method for error analysis in real time numeric algorithms, in: Proceedings of IMACS World Congress, Paris, France, 1988, pp. 706–709.